EISSN: 2707-0425

East African Journal of Science, Technology and Innovation, Vol. 7 (2): March 2026

Analysis of the spatial-temporal model for harvested predator-prey system with prey refuge and intraspecific competition

[1]NKULU, C. J., [*1]JAMES, M. N., [2]SAGAMIKO, T. D.

[*1]Department of Mathematics, College of Natural and Applied Sciences, University of Dar es Salaam, Tanzania.
[2]Department of Physics, Mathematics and Informatics, Dar es Salaam University College of Education, University of Dar es Salaam,Tanzania.

*Corresponding author: makungu_j@yahoo.com

Abstract

This study investigated the spatial-temporal dynamics of a predator-prey system incorporating prey refuge, intraspecific competition, harvesting, and diffusion. Spatial pattern formation in a predator-prey system governed by a reaction-diffusion framework was also considered. By incorporating spatial movement through diffusion, the non-spatial model by Mapunda and Sagamiko was extended into a partial differential equation (PDE) framework, enabling the analysis of self-organized spatial patterns such as spots and stripes that arose due to Turing instability. The coexistence equilibrium was analyzed for stability, and numerical simulations were performed using the Implicit-Explicit (IMEX) Euler method for time integration with the finite difference method employed for discretization of the Laplacian operator under Neumann boundary conditions (zero-flux), assuming no population flux across the boundary. The impact of key ecological parameters, particularly the refuge rate m and diffusion coefficients D_1 and D_2 on population distribution and pattern evolution was systematically explored. Simulation results revealed that increasing diffusion coefficients enhanced well-defined spatial aggregation of predators and prey while decreasing the refuge level intensified predation pressure and accelerated pattern formation. Specifically, when $D_2 > D_1$ (predators diffused faster than prey), the homogeneous coexistence equilibrium destabilized, leading to Turing-type patterns including isolated hotspots and periodic bands. At higher refuge levels such as $m = 0.9$ combined with elevated predator diffusion ($(D_2 \geq 0.9)$ the system exhibited stable and matured spot patterns, indicating a balance between protection and mobility. These findings highlight the critical role of species mobility and protective mechanisms in shaping ecosystem structure and offered important insights for conservation strategies and the sustainable management of harvested populations in spatially heterogeneous environments.

Key words: *Intraspecific competition; Predator; Prey; Prey refuge; Reaction-Diffusion; Turing instability*

Cite as: Nkulu *et al.* (2026): Analysis of the spatial-temporal model for harvested predator-prey system with prey refuge and intraspecific competition. *East African Journal of Science, Technology and Innovation, 7* (2).

Received: 07/01/26
Accepted: 30/03/26
Published: 30/03/26

Introduction

Predator-prey interactions are fundamental to ecological systems, influencing population dynamics, biodiversity and ecosystem stability (Berryman, 2000). Understanding these relationships is important for developing strategies to manage and conserve natural resources, particularly when accounting for factors such as prey refuge, harvesting, intraspecific competition and diffusion (Kar, 2005). Incorporating spatiotemporal dynamics into these models allows for a more accurate representation of population distributions and ecosystem stability (Cosner, 2004). While traditional models focus on direct interactions, recent spatiotemporal models incorporate additional mechanisms to better reflect real-world ecosystems (Sharmila e*t al.,* 2023).

Intraspecific competition occurs when individuals of the same species compete for limited resources, regulating population densities and preventing abrupt fluctuations (Das *et al.,* 2013).

Prey refuge provides safe zones that reduce predation risk, serving as a stabilizing mechanism that allows for long-term coexistence and prevents prey extinction (Kar, 2005; Majeed, 2018). In spatial frameworks, refuge distribution influences aggregation and diffusion patterns (Kumar, 2006; Han, 2021).

Harvesting, through human activities like hunting or fishing, impacts ecological balance in which sustainable techniques support stable levels while excessive harvesting can lead to collapse (Mapunda *et al.*, 2018; Quan *et al.,* 2023).

Diffusion represents individual movement within spatially structured environments. Studies demonstrate that differential diffusion rates play a critical role in shaping spatial patterns, where weak diffusion promotes heterogeneity and coexistence, while strong diffusion can homogenize populations (Mohd *et al.,* 2012; Liu *et al.,* 2019).

Although existing research has investigated these components individually or in pairs, few studies integrate all four mechanisms into a unified spatial framework. For instance, Sharmila *et al.* (2023) analyzed reaction-diffusion dynamics using weak nonlinear analysis, highlighting diffusion's influence, while Han *et al.* (2021) explored refuge and diffusion effects on stability. However, these studies often omit the combined impact of harvesting and intraspecific competition within a spatial context. This study addresses this gap by extending the non-spatial model of Mapunda and Sagamiko (2021) which considered refuge, competition, and harvesting into a reaction-diffusion system. By integrating prey refuge, intraspecific competition, harvesting, and diffusion into a single spatiotemporal model. This work provides a deeper understanding of how these factors interact to drive pattern formation and ecosystem resilience. This integrated approach offers improved insights for ecological management and conservation strategies in spatially heterogeneous environments.

Materials and Methods

Model formulation

This study formulated and analyzed a spatial-temporal predator-prey model extending the non-spatial system originally described by Mapunda and Sagamiko (2021). The extended model incorporated prey refuge *(m)*, intraspecific predator competition *(a),* harvesting *(h)* and diffusion coefficient $(\mathrm{Dq}, \mathrm{Dz})$. The model was subsequently non-dimensionalized to yield a dimensionless system governed by key parameters, including normalized harvesting refuge(m), competition coefficient (a_3), and diffusion coefficients. Theoretical analysis established solution boundedness, identified three biologically meaningful equilibria, and derived conditions for coexistence. Linear stability analysis revealed that the coexistence equilibrium (E_2) was locally asymptotically stable in the absence of diffusion but became susceptible to Turing instability when $\mathrm{D}_2 > \mathrm{D}_1$.

The simulations were conducted on a two-dimensional domain

$$[0, L_x]\times[0, L_y] = [0,100]\times[0,100] \quad (1)$$

with homogeneous Neumann (zero-flux) boundary conditions:

$$\frac{\partial q}{\partial \nu} = 0, \ \frac{\partial z}{\partial \nu} = 0, \ on \ \partial\Omega \quad (2)$$

which model a closed ecosystem where individuals can not enter or leave, ensuring ecological realism for isolated habitats such as reserves. Spatial discretization was performed using the five-point finite difference stencil. A uniform grid of size $N_x \times N_y$ = 128×128 yielded spatial steps $\Delta x = \Delta y \approx 0.787$, providing sufficient resolution to capture fine-scale patterns like spots and stripes while remaining computationally feasible. Initial conditions were set near the coexistence equilibrium $E_2(q^*, z^*)$, with small random perturbations of amplitude $\varepsilon = 0.1$ added to both prey and predator densities. This broke spatial symmetry and triggered pattern formation for the system susceptible to Turing instability.

All simulations were implemented in MATLAB

R2024a. Therefore, the current model extended this ODEs below.

$$\begin{cases} \frac{dq}{dt} = rq\left(1-\frac{q}{K}\right) - \beta_1(1-m)qz - hq \\ \frac{dz}{dt} = \beta_2(1-m)qz - \mu z - az^2 \end{cases} \quad (3)$$

Where q and z represent prey and predator densities respectively while all other parameters are defined in the table below.

Table 1

List of parameters used in the model and their implications

Parameter	Description
r	Intrinsic growth rate of the prey population.
K	Carrying capacity of the prey environment.
β_1	Predation rate coefficient (effect of predator on prey).
β_2	Conversion efficiency of prey into predator biomass.
m	Proportion of prey protected in the refuge.
h	Harvesting rate of the prey.
μ	Mortality rate of the predator.
a	Intraspecific competition coefficient among predators.
D_q	Diffusion coefficient of the prey.(measures how fast prey move)
D_z	Diffusion coefficient of the predator.(measures how fast predator move

From equation (1), the term $rq\left(1-\frac{q}{K}\right)$ represents the logistic growth of the prey population. The expression $-\beta_1(1-m)qz$ represents predation term which reduces the prey population over time because predators consume them while $-\beta_1$ is the predation rate which describes how efficiently predators consume prey.Parameter m indicates the fraction of prey that is safe from predation. Therefore, $(1-m)$ represents the fraction of exposed prey that are vulnerable to predation.

Where:

i. If $m = 0$ means no refuge (prey is fully exposed to predation).
ii. If $m = 1$ means there is full refuge (prey is completely protected, no predation occurs).
iii. If $0 < m < 1$ means there is partial refuge such that some prey are protected, but others are still vulnerable.

Therefore, the term $\beta_1(1-m)qz$ with negative (-) sign represents removal of prey due to predation. The term qz represents predator-prey interactions which defines how often predators and prey encounter each other. The term $-hq$ represents harvesting term in which h represents the rate at which prey are removed from the system due to harvesting by either human fishing, hunting or resource extraction.

On the other hand the term $\beta_2(1-m)qz$ represents the rate at which predators increase due to predation on the available (non-refuged) prey.

The term β_2 represents efficiency of converting consumed prey into predator births while $-\mu z$ represents natural mortality term. In this term, μ is a positive constant that denotes the per capita natural mortality rate of the predators. The term $-\mu z$ means that predators are dying at a rate proportional to their current population. Predator deaths may happen due to natural causes such as aging, disease or starvation.The term $-az^2$ represents intraspecific competition among predators while a is a positive constant that quantifies the strength of intraspecific

competition.

To address the gap in the existing model, the current study aims to extend model (3) by incorporating spatial components to the model equations, which changes the model equations (3) to Partial Differential equations (PDEs). This extension aims to allow analysis of how spatiotemporal factors such as diffusion, prey refuge, intraspecific competition and harvesting influence population distributions in the system.
The model formulated is partial differential equations (PDEs) that accounts for both temporal (time) aspect and spatial (space) dispersal of the populations.

The diffusion terms $D_q\nabla^2 q$ where $\nabla^2 q=\frac{\partial q^2}{\partial x^2}+\frac{\partial z^2}{\partial y^2}$ and $D_z\nabla^2 z$ where $\nabla^2 z=\frac{\partial z^2}{\partial x^2}+\frac{\partial z^2}{\partial y^2}$ account for space (x,y) in 2 dimensions, are added to prey and predator equations in model (3), respectively to capture the spatial-temporal dynamics and the current model becomes a PDE model as shown below;

$$\begin{cases} \frac{\partial q}{\partial t} = rq\left(1-\frac{q}{K}\right)-\beta_1(1-m)qz-hq+D_q\nabla^2 q, & X\in\Omega, t>0 \\ \frac{\partial z}{\partial t} = \beta_2(1-m)qz-\mu z-az^2+D_z\nabla^2 z, & X\in\Omega, t>0 \\ \frac{\partial q(X,t)}{\partial \nu}=\frac{\partial z(X,t)}{\partial \nu}=0, & X\in\partial\Omega, t>0 \\ q(X,0)=q_0(X)\geq 0,\ z(X,0)=z_0(X)\geq 0, & X\in\Omega \end{cases} \quad (4)$$

Where: $\partial q=\partial q(x,y,t)$ and $\partial z=\partial z(x,y,t)$ represent prey and predator densities at location (x, y) at time t, respectively.
In the 2-D context, the notation $X\in\Omega$, $t>0$ means $X=(x, y)$ is the position vector that lies within the spatial domain $\Omega\in R^2$. Also, time ($t>0$) is positive, the model describes the system's evolution after the initial time (usually $t=0$).
The expression $\frac{\partial q(X,t)}{\partial \nu}=\frac{\partial q(X,t)}{\partial \nu}=0$ is called the Neumann boundary condition, which biologically means no flux (in or out) of the quantities $q(X, t)$ and $z(X, t)$ across the boundary $\partial\Omega$. The conditions $q(X,0)=q_0(X)\geq 0$, $z(X,0)=z_0(X)\geq 0$, $X\in\Omega$ indicate that at the beginning of the process, the prey and predator populations are distributed across the habitat Ω with non-negative densities.

Boundedness of the solution

Population densities of living individuals cannot be negative or infinite in the real ecosystem. To show that $q(X, t)$ and $z(X, t)$ stay positive and finite for all time to ensure that the model respects biological constraints, the following lemma holds.

Lemma 1.1. *All solutions of the given system* (4) *are non-negative and bounded in* $R^2_+=\{(q,z):q>0,z>0\}$

Proof. Considering the equations of model (4) as given here below;

$$\frac{\partial q}{\partial t}=rq\left(1-\frac{q}{K}\right)-\beta_1(1-m)qz-hq+D_q\nabla^2 q,$$
$$\frac{\partial z}{\partial t}=\beta_2(1-m)qz-\mu z-az^2+D_z\nabla^2 z.$$

To prove for boundedness in R^2_+, $\left(D_q\nabla^2 q \text{ and } D_z\nabla^2 z\right)$ are excluded and the model becomes an ODEs system;

$$\begin{aligned} \frac{dq}{dt}&=rq\left(1-\frac{q}{K}\right)-\beta_1(1-m)qz-hq, \\ \frac{dz}{dt}&=\beta_2(1-m)qz-\mu z-az^2. \end{aligned} \quad (5)$$

Required to prove that $q(t)$ and $z(t)$ remain non-negative and uniformly bounded for all $t\geq 0$.

Let $P(q, z)$ be the function that combines q and z such that;

$$P(q,z)=q+\frac{\beta_1}{\beta_2}z, \quad (6)$$

where $P(q,z)$ is the total population of prey q and predator z, while β_1 and β_2 are interaction coefficients.

Now, differentiating (6) using chain rule with respect to time gives:

$$\frac{dP}{dt}=\frac{dq}{dt}+\frac{\beta_1}{\beta_2}\cdot\frac{dz}{dt} \quad (7)$$

Then, substituting $\frac{dq}{dt}$ and $\frac{dz}{dt}$ from (5) into (7) respectively gives;

$$\frac{dP}{dt}=\left[rq\left(1-\frac{q}{K}\right)-\beta_1(1-m)qz-hq\right]+\frac{\beta_1}{\beta_2}\cdot\left[\beta_2(1-m)qz-\mu z-az^2\right] \quad (*)$$

Upon simplifying equation (*), β_2 in the second term cancels out and hence yields:

$$\frac{dP}{dt}=rq\left(1-\frac{q}{K}\right)-\beta_1(1-m)qz-hq+\beta_1(1-$$

The terms $\beta_1(1-m)qz$ and $-\beta_1(1-m)qz$ in (8) cancel out which yields:

$$\frac{dP}{dt}=rq\left(1-\frac{q}{K}\right)-hq-\frac{\beta_1}{\beta_2}\left[\mu z+az^2\right]$$

Simplifying the term $rq\left(1-\frac{q}{K}\right)$ gives:

$$\frac{dP}{dt}=rq-\frac{rq^2}{K}-hq-\frac{\beta_1}{\beta_2}\left[\mu z+\alpha z^2\right]$$
$$\frac{dP}{dt}=(r-h)q-\frac{rq^2}{K}-\frac{\beta_1}{\beta_2}\left[\mu z+\alpha z^2\right] \quad (9)$$

Choosing an arbitrary constant, say ν, to modify the total population F such that νF. Then, upon adding νF to (9) both sides, results in;

$$\frac{dP}{dt}+vP=(r-\mathrm{h})q-\frac{rq^2}{K}-\frac{\beta_1}{\beta_2}[\mu z+\alpha z^2]+vP, \qquad (10)$$

Since;

$$P=q+\frac{\beta_1}{\beta_2}z \qquad (11)$$

Substituting (11) into (10) in the R.H.S only yields ;

$$\frac{dP}{dt}+vP=(r\text{-}\mathrm{h})q-\frac{rq^2}{K}-\frac{\beta_1}{\beta_2}\left[\mu z+\alpha z^2\right]+vq+\frac{\beta_1}{\beta_2}z \qquad (**)$$

upon simplifying equation (**) gives;

$$\frac{dP}{dt}+vP=(r\text{-}\mathrm{h})q-\frac{rq^2}{K}-\frac{\beta_1}{\beta_2}\left[\mu z+\alpha z^2\right]+vq+\frac{\beta_1}{\beta_2}z \qquad (***)$$

simplifying by collecting like terms together equation (***) gives;

$$\frac{dP}{dt}+vP=(r-\mathrm{h}+v)q-\frac{rq^2}{K}-\frac{\beta_1}{\beta_2}[\alpha z^2+(\mu-v)z]. \qquad (12)$$

R.H.S becomes quadratic in q such that $(r-\mathrm{h}+v)q-\frac{rq^2}{K}$ and quadratic in z such that $-\frac{\beta_1}{\beta_2}[\alpha z^2+(\mu-v)z]$.

Applying $\frac{4ac-b^2}{4a}$ for maximum value of $(r-\mathrm{h}+v)q-\frac{rq^2}{K}$ and $-\frac{\beta_1}{\beta_2}[\alpha z^2+(\mu-v)z]$ yields;

$$\mathrm{Max}\left[(r\text{-}\mathrm{h}+v)q-\frac{rq^2}{K}\right]=\frac{K(r\text{-}\mathrm{h}+v)^2}{4r} \qquad (****)$$

and

$$\mathrm{Max}\left[-\frac{\beta_1}{\beta_2}\left(\alpha z^2+(\mu\text{-}v)z\right)\right]=\frac{\beta_1(\mu\text{-}v)^2}{4\alpha\beta_2}. \qquad (*****)$$

Therefore, by combining (****) and (*****) the maximum value of R.H.S becomes;

$$\mathrm{Max}\left[(r-\mathrm{h}+v)q-\frac{rq^2}{K}-\frac{\beta_1}{\beta_2}(\alpha z^2+(\mu-v)z)\right]=\frac{K(r-\mathrm{h}+v)^2}{4r}+\frac{\beta_1(\mu-v)^2}{4\alpha\beta_2} \qquad (******)$$

By substituting R.H.S expression of (******) into equation (12), yields;

$$\frac{dP}{dt}+vP\le\frac{K(r-\mathrm{h}+v)^2}{4r}+\frac{\beta_1(\mu-v)^2}{4\alpha\beta_2} \qquad (13)$$

Let,

$$M=\frac{K(r-\mathrm{h}+v)^2}{4r}+\frac{\beta_1(\mu-v)^2}{4\alpha\beta_2}.$$

Then, (13) becomes;

$$\frac{dP}{dt}+vP\le M \qquad (14)$$

Upon integrating (14) using the integrating factor $I=e^{vt}$ and multiplying it by $I=e^{vt}$ throughout, yields;

$$e^{vt}\frac{dP}{dt}+e^{vt}vP\le Me^{vt} \qquad (15)$$

L.H.S becomes a derivative of $e^{vt}P$, then;

$$\frac{d}{dt}\left(e^{vt}P\right)\le Me^{vt} \qquad (16)$$

upon integrating (16) both sides taking the limits from 0 to t, gives

$$\int_0^t\frac{d}{ds}\left(e^{vs}P(s)\right)ds\le\int_0^t Me^{vs}ds \qquad (17)$$

After integrating both sides and taking the limits, (17) gives;

$$e^{vt}P(t)\le P(0)+\frac{M}{v}(e^{vt}\text{-}1). \qquad (18)$$

Now, rearranging (18) gives

$$e^{vt}P(t)-P(0)\le\frac{M}{v}(e^{vt}-1). \qquad (19)$$

Dividing (19) by e^{vt} both sides gives

$$P(t)\le P(0)e^{-vt}+\frac{M}{v}(1-e^{-vt})$$

As $t\to\infty$, the exponential term $e^{-vt}\to 0$, so:

$$P(t)\le P(0).0+\frac{M}{v}(1-0) \qquad (21)$$

Then; $P(t)\le\frac{M}{v}$

Therefore, $P(t)\le\frac{M}{v}$ becomes $P(q,z)\le\frac{M}{v}$ which is bounded below by 0 and above by $\frac{M}{v}$ such that $0\le P(q,z)\le\frac{M}{v}$

This shows both q and z are non-negative and uniformly bounded such that; $0\le q\le\frac{M}{v}$ and $0\le z\le\frac{M}{v}$.

Hence, this completes the proof.

Existence of equilibrium points

To determine the equilibrium points of the model equations (4) diffusion parts are temporarily excluded from the model equations, which implies the diffusion parts become zero.

When diffusion parts are excluded, the model equations reduce to the following system of ordinary differential equations (ODEs):

$$\begin{cases}\frac{dq}{dt}=rq\left(1-\frac{q}{K}\right)-\beta_1(1-m)qz-\mathrm{h}q\\ \frac{dz}{dt}=\beta_2(1-m)qz-\mu z-\alpha z^2,\end{cases} \qquad (22)$$

To find the equilibrium points of the model equations (22), the time derivatives $\frac{dq}{dt}$ and $\frac{dz}{dt}$ are set to zero and solve the resulting algebraic system:

$$\begin{cases} 0 = rq\left(1-\frac{q}{K}\right)-\beta_1(1-m)qz-\mathrm{h}q \\ 0 = \beta_2(1-m)qz-\mu z-\alpha z^2 \end{cases} \quad (23)$$

Physically, the equilibrium points represent constant population densities where neither the prey (q) nor the predator (z) changes over time.

Now, assuming a trial equilibrium point (q^*, z^*), where the time derivatives of both prey and predator populations are zero: $\frac{dq}{dt}=0$, $\frac{dz}{dt}=0$.

$$\begin{cases} rq^*\left(1-\frac{q^*}{K}\right)-\beta_1(1-m)q^*z^*-\mathrm{h}q^*=0 \\ \beta_2(1-m)q^*z^*-\mu z^*-\alpha(z^*)^2=0 \end{cases} \quad (24)$$

The system (24) above gives the trivial equilibrium point E_0 = (0,0), which means both species extinct (disappear). This can happen due to over-harvesting or disease and the ecosystem can completely collapse.

Upon substituting z^* (zero predator) into the prey equation, it gives q^*:

$0=rq^*\left(1-\frac{q^*}{K}\right)-\mathrm{h}q^*$.

Here, either $q^*=0$ or $q^*=K\left(1-\frac{\mathrm{h}}{K}\right)$

Considering $q^*=K\left(1-\frac{\mathrm{h}}{K}\right)$, the prey-only equilibrium becomes:

$E_1=\left(K\left(1-\frac{\mathrm{h}}{K}\right),0\right)$, $r>\mathrm{h}$ which exists if harvesting does not exceed the prey's intrinsic growth rate. This means prey survive in the absence of predators.

For coexistence Equilibrium $(q^*>0,\ z^*>0)$.

Consider the model equations below,

$$\begin{cases} rq^*\left(1-\frac{q^*}{K}\right)-\beta_1(1-m)q^*z^*-\mathrm{h}q^*=0, \\ \beta_2(1-m)q^*z^*-\mu z^*-\alpha(z^*)^2=0. \end{cases} \quad (25)$$

Solving for z^* from $\beta_2(1-m)q^*z^*-\mu z^*-\alpha(z^*)^2=0$. it gives,

$$z^*=\frac{\beta_2(1-m)q^*-\mu}{\alpha}. \quad (26)$$

Substituting (26) into $rq^*\left(1-\frac{q^*}{K}\right)-\beta_1(1-m)q^*z^*-\mathrm{h}q^*=0$ gives

$$q^*=\frac{r+\frac{\beta_1(1-m)\mu}{\alpha}-\mathrm{h}}{\frac{r}{K}+\frac{\beta_1\beta_2(1-m)^2}{\alpha}}$$

Upon simplifying q^* gives;

$$q^*=\frac{K\alpha(r-\mathrm{h})+\mu K\beta_1(1-m)}{r\alpha+K\beta_1\beta_2(1-m)^2} \quad (27)$$

Then substitute (27) into (26), z^* becomes;

$$z^*=\frac{\beta_2(1-m)}{\alpha}\cdot\left(\frac{K\alpha(r-\mathrm{h})+K\beta_1(1-m)\mu}{r\alpha+K\beta_1\beta_2(1-m)^2}\right)-\frac{\mu}{\alpha}.$$

Upon simplifying z^*, yields ;

$$z^*=\frac{1}{\alpha}\left[\frac{K\alpha\beta_2(1-m)(r-\mathrm{h})+K\beta_1\beta_2(1-m)^2\mu-\mu r\alpha-\mu K\beta_1\beta_2(1-m)^2}{r\alpha+K\beta_1\beta_2(1-m)^2}\right]$$

Notice that the terms involving $K\beta_1\beta_2(1-m)^2\mu$ cancel out, and after further simplification, finally z^* becomes: $z^*=\frac{K\beta_2(1-m)(r-\mathrm{h})-\mu r}{r\alpha+K\beta_1\beta_2(1-m)^2}$.

Therefore;

$$(q^*,z^*)=\left(\frac{K\alpha(r-\mathrm{h})+K\beta_1(1-m)\mu}{r\alpha+K\beta_1\beta_2(1-m)^2},\ \frac{K\beta_2(1-m)(r-\mathrm{h})}{r\alpha+K\beta_1\beta_2(1-m}\right.$$

Hence:

$$E_2=\left(\frac{K\alpha(r-\mathrm{h})+K\beta_1(1-m)\mu}{r\alpha+K\beta_1\beta_2(1-m)^2},\frac{K\beta_2(1-m)(r-\mathrm{h})-\mu r}{r\alpha+K\beta_1\beta_2(1-m)^2}\right)$$

This is a coexistence equilibrium point in which both predator and prey exist, and it exists only if $q^*>0$ and $z^*>0$ where $r>\mathrm{h}$ and $0\le m<1-\frac{r(\mu)}{K\beta_2(r-\mathrm{h})}$

This represents a balanced ecosystem where prey grow but are controlled by predation and harvesting. On the other hand, predators survive due to successful predation, but are limited by natural death and intraspecific competition. This equilibrium point is especially interesting because it shows how both species can coexist over the long term. The coexistence equilibrium point gives an understanding of how ecosystems maintain balance.

Linear stability analysis

The stability analysis of each equilibrium point is performed by computing the Jacobian matrix of system (4) and using the eigenvalues of the Jacobian matrix to determine the stability condition. By using equilibrium points of the Jacobian matrix, the point is asymptotically stable if the real parts of the eigenvalues of each Jacobian matrix are negative and unstable if otherwise.

From the system of equations:

$$\begin{cases} \frac{dq}{dt}=rq\left(1-\frac{q}{K}\right)-\beta_1(1-m)qz-\mathrm{h}q, \\ \frac{dz}{dt}=\beta_2(1-m)qz-\mu z-\alpha z^2. \end{cases}$$

To find the Jacobian matrix, let:

$$f(q,z)=rq\left(1-\frac{q}{K}\right)-\beta_1(1-m)qz-\mathrm{h}q,$$

$$g(q,z)=\beta_2(1-m)qz-\mu z-\alpha z^2$$

The Jacobian matrix of (28) is calculated using:

$$J(q,z)=\begin{bmatrix} \frac{\partial f}{\partial q} & \frac{\partial f}{\partial z} \\ \frac{\partial g}{\partial q} & \frac{\partial g}{\partial z} \end{bmatrix}$$

Then, the Jacobian matrix becomes:

$$J(E_i)=\begin{bmatrix} r\left(1-\frac{2q}{K}\right)-\beta_1(1-m)z-\mathrm{h} & -\beta_1(1-m)q \\ \beta_2(1-m)z & \beta_2(1-m)q-\mu-2\alpha z \end{bmatrix} \quad (29)$$

Now, to analyze the stability of equilibrium points, the Jacobian matrix is evaluated at each equilibrium point as follows,

(i) $E_0=(0,0)$

The Jacobian matrix evaluated at $E_0=(0,0)$ becomes;

$$J(q,z)=\begin{bmatrix} r-\mathrm{h} & 0 \\ 0 & -\mu \end{bmatrix}$$

The eigenvalues of the Jacobian matrix evaluated at the trivial equilibrium point $E_0=(0,0)$ are; $\lambda_1=r-\mathrm{h}$, $\lambda_2=-\mu$

where, $\lambda_2=-\mu<0$ is always negative because μ is a positive constant and $\lambda_1=r-\mathrm{h}>0$ gives $r>\mathrm{h}$ (which implies that growth rate of prey should be greater than the harvesting rate) in which prey grows away from extinction, and hence E_0 (0,0)is unstable.

(ii) $E_1=\left(K\left(1-\frac{\mathrm{h}}{r}\right),0\right)$

The Jacobian matrix evaluated at E_1 is given as:

$$J(E_1)=\begin{bmatrix} (r-\mathrm{h}) & -\beta_1(1-m)K\left(1-\frac{\mathrm{h}}{r}\right) \\ 0 & \beta_2(1-m)K\left(1-\frac{\mathrm{h}}{r}\right)-\mu \end{bmatrix}$$

Eigenvalues of the Jacobian matrix $J(E_1)$ are:

$$\lambda_1=-(r-\mathrm{h}),\ \lambda_2=\beta_2(1-m)K\left(1-\frac{\mathrm{h}}{r}\right)-\mu$$

Here, if $\lambda_1=-(r-\mathrm{h})<0$ ($r>\mathrm{h}$ always, then $(r-\mathrm{h})$ is positive and hence $\lambda_1<0$)(negative) , this means that prey grow, but on the other hand, if $-(r-\mathrm{h})>0$ means $r<\mathrm{h}$ violates biological and ecosystem balance because prey decline.

Thus, $\lambda_1<0$ for prey to exist.

Also $\lambda_2=\beta_2(1-m)K\left(1-\frac{\mathrm{h}}{r}\right)-\mu>0$

Here $\beta_2(1-m)K\left(1-\frac{\mathrm{h}}{r}\right)>\mu$ means the growth rate of the predator population (from feeding on prey) exceeds their natural death rate (μ), and predators can invade (a small number of predators introduced into a prey-only environment can successfully grow in number and establish themselves in the system). The available prey not in refuge is sufficient to allow the predator population to grow. This makes the prey-only equilibrium point E_1 unstable, and predators will establish themselves in the system. On the other hand, if $\lambda_2<0$ such that $\beta_2(1-m)K\left(1-\frac{\mathrm{h}}{r}\right)<\mu$ then predators cannot invade, they die off if introduced.

(iii)

$$E_2=\left(\frac{K\alpha(r-\mathrm{h})+K\beta_1(1-m)\mu}{r\alpha+K\beta_1\beta_2(1-m)^2},\frac{K\beta_2(1-m)(r-\mathrm{h})-\mu r}{r\alpha+K\beta_1\beta_2(1-m)^2}\right)$$

Jacobian matrix of the coexistence equilibrium point E_2 takes the form:

$$\mathrm{J}(E_2)=\begin{bmatrix} \mathrm{A} & \mathrm{B} \\ \mathrm{C} & \mathrm{D} \end{bmatrix}$$

Where

$$\mathrm{A}=-\left[\frac{2r[\alpha(r-\mathrm{h})-\beta_1(m-1)\mu]+\beta_1(m-1)[K\beta_2(\mathrm{m}\text{-}1)(r-\mathrm{h})-\mu r]+(r-\mathrm{h})(r\alpha+K\beta_1\beta_2(m-1)^2)}{r\alpha+K\beta_1\beta_2(m-1)^2}\right]$$

Where $r-\mathrm{h}>0$(always positive) (since $r>\mathrm{h}$ for prey to exist) and $(1-m)>0$ (positive) (since $0\le m<1$), therefore A < 0 with specific parameter values in Table 2.

$$\mathrm{B}=-\left[\frac{\beta_1(1-m)(K\alpha(r-\mathrm{h})+K\beta_1(1-m)\mu)}{r\alpha+K\beta_1\beta_2(1-m)^2}\right]$$

Since (1−m)>0 (positive), B < 0 with specific parameter values in Table 2.

$$\mathrm{C}=\frac{\beta_2(1-m)[K\alpha(r-\mathrm{h})+K\beta_1(1-m)\mu]}{r\alpha+K\beta_1\beta_2(1-m)^2}$$

Since (1−m)>0 (positive), C > 0 with specific parameter values in Table 2.

$$\mathrm{D}=\frac{\beta_2(1-m)[K\alpha(r-\mathrm{h})+K\beta_1(1-m)\mu]}{r\alpha+K\beta_1\beta_2(1-m)^2}-\frac{\mu[r\alpha+K\beta_1\beta_2(1-m)^2]}{r\alpha+K\beta_1\beta_2(1-m)^2}-\frac{2\alpha[K\beta_2(1-m)(r-\mathrm{h})-\mu r]}{r\alpha+K\beta_1\beta_2(1-m)^2}$$

Suppose the Jacobian matrix (30) has the following characteristic polynomial equation below:

$$\lambda^2-(A+D)\lambda+(AD-BC)=$$

Then, the stability of equilibrium E_2 is stated by using the trace and determinant criteria of the Jacobian matrix (31) as follows:

$$Tr(J(E_2))=A+D$$
$$Det(J(E_2))=AD-BC$$

Since:

$A<0$, $B<0$ and $C>0$ then the linear stability of the coexistence equilibrium point E_2 is locally asymptotically stable **if** $D<0$ (for all parameter values in Table 2) which yields:

$$Tr(J(E_2))=A+D<0$$

$$Det(J(E_2))=AD-BC>0$$

The stability of the coexistence equilibrium point (interior points) such that $q^* > 0$ indicates that there is a positive prey population at equilibrium, while $z^* > 0$, shows that the predator population is positive at equilibrium. Small perturbations (temporary changes in population sizes due to environmental fluctuations) will not lead to extinction, which implies that both species coexist in the long run and neither of them will become extinct.

The prey and predator populations stabilize at constant positive levels, which reflects a balance between prey growth and predation pressure. Also ecosystem can sustain both species over time under current environmental conditions and parameter values.

Existence of periodic solution

To check whether the system (4) has periodic solutions, the diffusion parts are excluded, and then the system becomes an ordinary differential equation as follows:

$$\begin{cases} \frac{dq}{dt} = rq\left(1-\frac{q}{K}\right) - \beta_1(1-m)qz - \mathrm{h}q, \\ \frac{dz}{dt} = \beta_2(1-m)qz - \mu z - \alpha z^2 \end{cases} \quad (32)$$

Then, let: $\frac{dq}{dt} = f(q,z)$ and $\frac{dz}{dt} = q(q,z)$

Where:

$f(q,z) = rq\left(1-\frac{q}{K}\right) - \beta_1(1-m)qz - \mathrm{h}q$ and

$g(q,z) = \beta_2(1-m)qz - \mu z - \alpha z^2$

To check the existence of periodic solutions, Bendixson's Negative Criterion is applied to check whether there is a change in sign (positive or negative), and if so:

$$\frac{\partial f}{\partial q} = \frac{\partial}{\partial q}\left[rq\left(1-\frac{q}{K}\right) - \beta_1(1-m)qz - \mathrm{h}q\right]$$

$$\frac{\partial f}{\partial q} = r\left(1-\frac{2q}{K}\right) - \beta_1(1-m)z - \mathrm{h} \quad \text{.....(a)}$$

$$\frac{\partial g}{\partial z} = \frac{\partial}{\partial z}[\beta_2(1-m)qz - \mu z - \alpha z^2]$$

$$\frac{\partial g}{\partial z} = \beta_2(1-m)q - \mu - 2\alpha z \quad \text{.....(b)}$$

Upon adding (a) and (b), yields;

$$\frac{\partial f}{\partial q} + \frac{\partial g}{\partial z} = \left[r\left(1-\frac{2q}{K}\right) - \beta_1(1-m)z - \mathrm{h}\right] + [\beta_2(1-m)q - \mu - 2\alpha z],$$

$$\frac{\partial f}{\partial q} + \frac{\partial g}{\partial z} = (r - \mathrm{h} - \mu) + \left(\beta_2(1-m) - \frac{2r}{K}\right)q + (-\beta_1(1-m) - 2\alpha)z.$$

Therefore;

$$\frac{\partial f}{\partial q} + \frac{\partial g}{\partial z} = (r - \mathrm{h} - \mu) + \left(\beta_2(1-m) - \frac{2r}{K}\right)q + (-\beta_1(1-m) - 2\alpha)z. \quad (33)$$

Theorem 1.1 (Bendixson's Negative Criterion)

If the divergence of the vector field, $\frac{\partial f}{\partial q} + \frac{\partial g}{\partial z}$ *does not change sign and is not identically zero in a simply connected region of the phase plane, then the system has no closed orbits (periodic solutions) in that region.*

According to Bendixson's Negative Criterion, stated in the Theorem 1.1 above, equation (33) is not zero, such $\frac{\partial f(q,z)}{\partial q} + \frac{\partial g(q,z)}{\partial z} \neq 0$ and it changes sign with the parameter values in the Table 2, therefore; using the baseline parameter values in Table 2, the system (33) yields

$\frac{\partial f}{\partial q} + \frac{\partial g}{\partial z} = 0.5 - 1.5q - 0.7z$ which implies that equation (33) changes sign and not zero, therefore, by Bendixson's Negative Criterion, it is inconclusive.

Non-dimensionalization of the model

In this section, the dimensional model equations were transformed into dimensionless form for further analysis. Here, the physical units were eliminated, and the number of parameters was reduced by introducing the dimensionless variables. To analyze the spatiotemporal dynamics of the predator-prey system with prey refuge, harvesting, intraspecific competition, and diffusion, the model was non-dimensionalized to reduce complexity. This allowed to study the spatial population distribution of both species and Turing pattern formation, such as spots and stripes, under varying ecological conditions using fewer and more interpretable parameters.

Considering the model equations (4) as given below

$$\begin{cases} \frac{\partial q}{\partial t} = rq\left(1-\frac{q}{K}\right) - \beta_1(1-m)q \\ \frac{\partial z}{\partial t} = \beta_2(1-m)qz - \mu z - \alpha \\ \frac{\partial q(X,t)}{\partial \nu} = \frac{\partial z(X,t)}{\partial \nu} = \\ q(X,0) = q_0(X) \geq 0,\ z(X, \end{cases}$$

Now, to transform this model, let non-dimensional variables be:

$q^* = \frac{q}{K}$: Prey scaled by carrying capacity.

$z^* = \frac{\beta_1 z}{r}$: Predator scaled by $\frac{r}{\beta_1}$

$t^* = rt$: Time scaled by prey growth rate.

$x^* = \frac{x}{L}$, $z^* = \frac{y}{L}$: Space scaled by domain size.

Now, each derivative and terms are expressed in terms of starred variables as follows:

For q: $q^* = \frac{q}{K} \rightarrow q = q^* K$

Then, by applying the chain rule, this results in;

$$\frac{\partial q}{\partial t} = \frac{\partial(q^* K)}{\partial t} = K\frac{\partial q^*}{\partial t^*} \cdot \frac{dq^*}{dt^*}$$

But $t^* = rt$ then $\frac{dq^*}{dt^*} = r$

So;

$$\frac{\partial q}{\partial t} = Kr\frac{\partial q^*}{\partial t^*}.$$

Similarly for z:

$$z^* = \frac{\beta_1 z}{r} \rightarrow z = \frac{r}{\beta_1} z^*$$

Then;

$$\frac{\partial z}{\partial t} = \frac{r^2}{\beta_1}\frac{\partial z^*}{\partial t^*} \quad (35)$$

The Laplacian operator transforms as:

$$\nabla^2 = \frac{\partial^2}{\partial x^2} + \frac{\partial^2}{\partial y^2} = \frac{1}{L^2}\left(\frac{\partial^2}{\partial x^{*2}} + \frac{\partial^2}{\partial y^{*2}}\right) \quad (36)$$

Then:

$$\nabla^2 = \frac{1}{L^2}\nabla^{*2}.$$

Diffusion parts are transformed as follows;

For q:

$$D_q\nabla^2 q = D_q\nabla^2(Kq^*) = D_q K\cdot\frac{1}{L^2}\nabla^{*2}q^*.$$

Then:

$$D_q\nabla^2 q = \frac{KD_q}{L^2}\nabla^{*2}q^*.$$

For z:

$$D_z\nabla^2 z = D_z\nabla^2\left(\frac{r}{\beta_1}z^*\right) = D_z\cdot\frac{r}{\beta_1}\cdot\frac{1}{L^2}\nabla^{*2}z^*$$

Then:

$$D_z\nabla^2 z = \frac{rD_z}{\beta_1 L^2}\nabla^{*2}z^* \quad (38)$$

From the prey equation, such that,

$$\frac{\partial q}{\partial t} = rq\left(1-\frac{q}{K}\right) - (1-m)qz - \mathrm{h}q + D_q\nabla^2 q \quad (39)$$

Whereby each term in (39) is now expressed in starred form as follows:

$$\frac{\partial q}{\partial t} = Kr\frac{\partial q^*}{\partial t^*}$$

$$rq\left(1-\frac{q}{K}\right) = r(Kq^*)(1-q^*) = rKq^*(1-q^*)$$

$$\beta_1(1-m)qz = \beta_1(1-m)(Kq^*)\left(\frac{r}{\beta_1}z^*\right) = r(1-m)Kq^*z^*$$

$$\mathrm{h}q = \mathrm{h}Kq^* \quad (34)$$

$$D_q\nabla^2 q = \frac{KD_q}{L^2}\nabla^{*2}q^*$$

Now, each term is substituted into equation (39), which then yields;

$$Kr\frac{\partial q^*}{\partial t^*} = rKq^*(1-q^*) - r(1-m)Kq^*z^* - \mathrm{h}Kq^* + \frac{KD_q}{L^2}\nabla^{*2}q^*. \quad (40)$$

Upon dividing (40) by Kr on both sides, the result is:

$$\frac{\partial q^*}{\partial t^*} = q^*(1-q^*) - (1-m)q^*z^* - \frac{\mathrm{h}}{r}q^* + \frac{D_q}{rL^2}\nabla^{*2}q^* \quad (41)$$

Now, define the followig:

$$r_1 = \frac{\mathrm{h}}{r},\ D_1 = \frac{D_q}{rL^2}.$$

Then (41) becomes;

$$\frac{\partial q^*}{\partial t^*} = q^*(1-q^*) - (1-m)q^*z^* - r_1q^* + D_1\nabla^{*2}q^* \quad (42)$$

From the predator equation

$$\frac{\partial z}{\partial t} = \beta_2(1-m)qz - \mu z - \alpha z^2 + D_z\nabla^2 z. \quad (43)$$

Similarly, upon substituting each starred term such that;

$$\frac{\partial z}{\partial t} = \frac{r^2}{\beta_1}\frac{\partial z^*}{\partial t^*} \quad (37)$$

$$\beta_2(1-m)qz = \beta_2(1-m)(Kq^*)\left(\frac{r}{\beta_1}z^*\right) = \frac{\beta_2 Kr}{\beta_1}(1-m)q^*z^*$$

$$\mu z = \mu\cdot\frac{r}{\beta_1}z^*$$

$$\alpha z^2 = \alpha\left(\frac{r}{\beta_1}z^*\right)^2 = \frac{\alpha r^2}{\beta_1^2}z^{*2},$$

$$D_z\nabla^2 z = \frac{rD_z}{\beta_1 L^2}\nabla^{*2}z^*,$$

Into equation (43) gives

$$\frac{r^2}{\beta_1}\frac{\partial z^*}{\partial t^*} = \frac{\beta_2 Kr}{\beta_1}(1-m)q^*z^* - \frac{\mu r}{\beta_1}z^* - \frac{\alpha r^2}{\beta_1^2}z^{*2} + \frac{rD_z}{\beta_1 L^2}\nabla^{*2}z^*. \quad (44)$$

Multiplying (44) by $\frac{\beta_1}{r^2}$ both sides gives;

$$\frac{\partial z^*}{\partial t^*} = \frac{\beta_2 K}{\beta_1}(1-m)q^*z^* - \frac{\mu}{r}z^* - \frac{\alpha r}{\beta_1}z^{*2} + \frac{D_z}{rL^2}\nabla^{*2}z^*. \quad (45)$$

By defining the following terms:

$a_1=\frac{\beta_2 K}{\beta_1}$, $a_2=\frac{\mu}{r}$, $a_3=\frac{\alpha r}{\beta_1}$, $D_2=\frac{D_z}{rL^2}$.

Then (45) becomes;

$$\frac{\partial z^*}{\partial t^*}=a_1(1-m)q^*z^*-a_2z^*-a_3z^{*2}+D_2\nabla^{*2}z^*. \qquad (46)$$

Now, combining (42) and (46) gives final dimensionless model equations with stars as follows.

$$\begin{cases} \dfrac{\partial q^*}{\partial t^*}=q^*(1-q^*)-(1-m)q^*z^*-r_1q^*+D_1\nabla^{*2}q^*, \\ \dfrac{\partial z^*}{\partial t^*}=a_1(1-m)q^*z^*-a_2z^*-a_3z^{*2}+D_2\nabla^{*2}z^*, \\ \dfrac{\partial q^*}{\partial \nu^*}=\dfrac{\partial z^*}{\partial \nu^*}=0 \\ q^*(x^*,y^*,0)=q_0^*(x^*,y^*)\geq 0, z^*(x^*,y^*,0)=z_0^*(x^*,y^*)\geq 0 \end{cases} \qquad (47)$$

After dropping stars, the final dimensionless model equations become:

$$\begin{cases} \dfrac{\partial q(x,t)}{\partial t}=q(1-q)-(1-m)qz-r_1q+D_1\nabla^2q, & x\in\Omega, t>0, \\ \dfrac{\partial z(x,t)}{\partial t}=a_1(1-m)qz-a_2z-a_3z^2+D_2\nabla^2z, & x\in\Omega, t>0, \\ \dfrac{\partial q(x,t)}{\partial \nu}=\dfrac{\partial z(x,t)}{\partial \nu}=0, & x\in\partial\Omega, t>0 \\ q(x,0)=q_0(x)\geq 0, \quad z(x,0)=z_0(x)\geq 0, & x\in\Omega \end{cases} \qquad (48)$$

Whereby:

$r_1=\frac{h}{r}$, $D_1=\frac{D_q}{rL^2}$, $a_1=\frac{\beta_2 K}{\beta_1}$, $a_2=\frac{\mu}{r}$, $a_3=\frac{\alpha r}{\beta_1}$, $D_2=\frac{D_z}{rL^2}$.

The system (48) admits three biological equilibrium points in the absence of diffusion:

1. *Trivial equilibrium:*

$E_0 = (0, 0)$

Represents the total extinction of both species. Linear stability analysis shows that E_0 is unstable when $r_1 < 1$, meaning prey can grow from arbitrarily low densities if harvesting is not excessive.

2. *Prey-only equilibrium:*

$E_1 = (1 - r_1, 0)$, exists if $r_1<1$

This is an unstable equilibrium point and describes a situation where predators can not sustain themselves and go extinct.

3. *Coexistence equilibrium:*

$E_2=\left(\frac{a_2(1-m)+a_3(1-r_1)}{a_1(1-m)^2+a_3}, \frac{(1-m)(1-r_1)a_1-a_2}{a_1(1-m)^2+a_3}\right)$ exists if and only if $(1-m)(1-r_1)a_1>a_2$

This condition ensures that predation is strong enough to support predator populations despite refuge effects and harvesting. Linear stability analysis of the corresponding ordinary differential equation (ODE) system as revealed earlier that the coexistence equilibrium E_2 is locally asymptotically stable under biologically realistic parameters. Thus, in a well-mixed (homogeneous) environment, small perturbations around E_2 decay over time, leading the system back to uniform coexistence.

However, introducing spatial diffusion fundamentally alters this behavior. Even when E_2 is stable in the absence of diffusion, it may become unstable if diffusion rates are unequal, particularly when predators diffuse faster than prey ($D_2 > D_1$). This phenomenon, known as diffusion-driven or Turing instability, arises because predators enhance locally while predators exert long-range suppression through rapid diffusion.

The parameter values used were dimensionless derived from ecological literature and they were chosen to illustrate the qualitative dynamical behavior of system (48), as summarized in Table 2 below.

Table 2

Parameter values for the model system (48)

Parameter	Value	Source
m	$0 \leq m < 1$	Standard range for refuge
r_1	0.5	(Kar *et al*., 2010)
D_1	0.1	(Hau *et al*., 2019)
D_2	0.2	(Hau *et al*., 2019)
a_1	0.1	(Sharmila *et al*., 2023)
a_2	0.02	(Renji *et al*., 2021)
a_3	0.3	(Sharmila *et al*., 2023)

Numerical simulations were performed using baseline parameters from different literature with a series of plots to illustrate the emergent spatial patterns over time. By slightly perturbing the initial uniform state near the coexistence equilibrium E_2, diverse population distributions were observed, such as isolated high-density prey regions, yellow periodic bands of high and blue low density, together with intricate interconnected patches. These distributions arise purely from diffusion-driven instabilities and reflect the self-organizing capacity of the ecosystem. Subsequent simulation plots also explored how variations in D_2 and m shift the system between different pattern types. This revealed transitions from stable coexistence to fragmented spatial distributions. The simulation plots to validate analytical data were carried out using parameter values from Table 2, together with total time steps that run from T = 500 to T = 10000, where spatial patterns depict well-defined predator and prey zones as T increases. Domain size $L_x = L_y = 100$, together with grid size $N_x \times N_y = 128 \times 128$. To ensure the system maintains its biological realism, the random perturbation of $\varepsilon = 0.1$ was chosen to ensure no uniform population distributions as the system evolves.

Results

Analytical studies analyzed in the previous section are not complete until the numerical simulations are carried out. In this section, different numerical analyses were done to validate the analytical solutions presented in the previous section.

Initially, populations begin to deviate from their initial near-uniform distribution with small perturbations, which start to grow due to diffusion-driven instability. The prey exhibits the formation of incipient high-density regions, while the predator density begins to reorganize in response, showing signs of aggregation in certain areas with prey and depletion in others. As time progresses, these transient structures gradually sharpen into well-defined and attain stable configurations.

Figure 1, with t = 50, displays uniformly distributed prey in hotspots surrounded by low-density zones and predators cluster in spatially correlated patches reflecting a balance between consumption, reproduction, competition, and dispersal. This progression illustrates how local species interactions combined with differential movement can generate complex spatial heterogeneity, even in a homogeneous environment.

Figure 1

Spatiotemporal Distribution of Predator and Prey with $D_1 = 0.1$ *and* $D_2 = 0.2$ *and* $t = 50$.

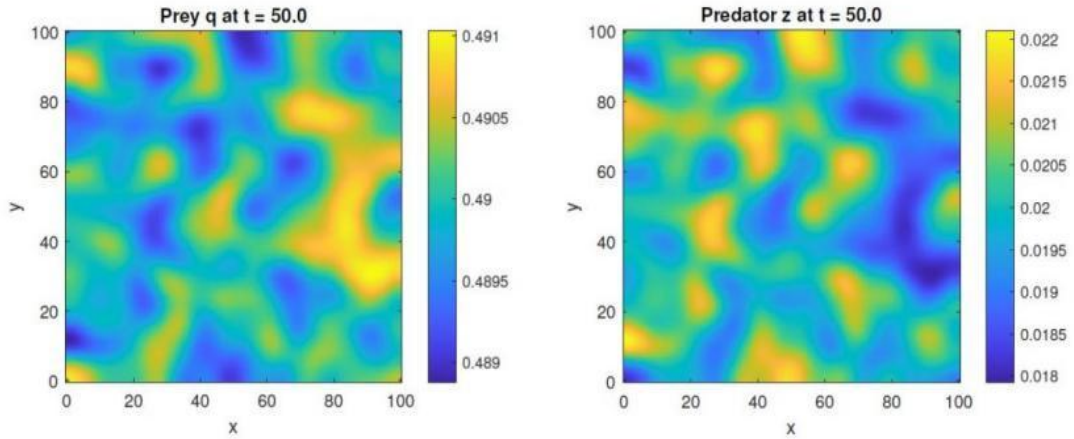

Note: Other parameter values used; $m = 0.5$, $r_1 = 0.5$, $a_1 = 0.1$, $a_2 = 0.02$, $a_3 = 0.3$

Figure 1 reveals the progressive development of spatial distribution in a predator-prey system driven by reaction-diffusion dynamics. Initially, prey distribution in the left plot begins to break symmetry from its initial uniform state, with some variations emerging across the domain. Regions highlighted in yellow and orange indicate aggregations of prey, with localized hotspots, while shades of blue reflect areas of lower density where depletion and dispersal dominate. The variation in prey densities arises due to different diffusion rates, where predators move faster than prey ($D_2 > D_1$), destabilizing the homogeneous coexistence equilibrium E_2. The predator population responds dynamically to the changes in prey distribution, where intense yellow regions reveal clusters of predators in proximity to prey aggregations, whereas deep blue zones denote the absence of predators. Over time, these transient fluctuations evolve into well-defined and stable spot patterns. Predators aggregate into corresponding clusters, aligning partially with prey hotspots but exhibiting internal competition that limits overaccumulation. These outcomes are shaped by biologically meaningful parameters such as diffusion rate $D_1 = 0.1$ and $D_2 = 0.2$, moderate harvesting pressure ($r_1 = 0.5$), partial refuge rate ($m = 0.5$), efficient predation ($a_1 = 0.1$), low predator mortality ($a_2 = 0.02$), and strong intraspecific competition ($a_3 = 0.3$). Homogeneous Neumann boundary conditions ensure no artificial flux at domain edges that tends to preserve mass and model a closed ecosystem, such as a protected reserve.

Figure 2

Spatiotemporal Distribution of Predator and Prey with $D_1 = 0.2$ *and* $D_2 = 0.5$ *and* $t = 100$.

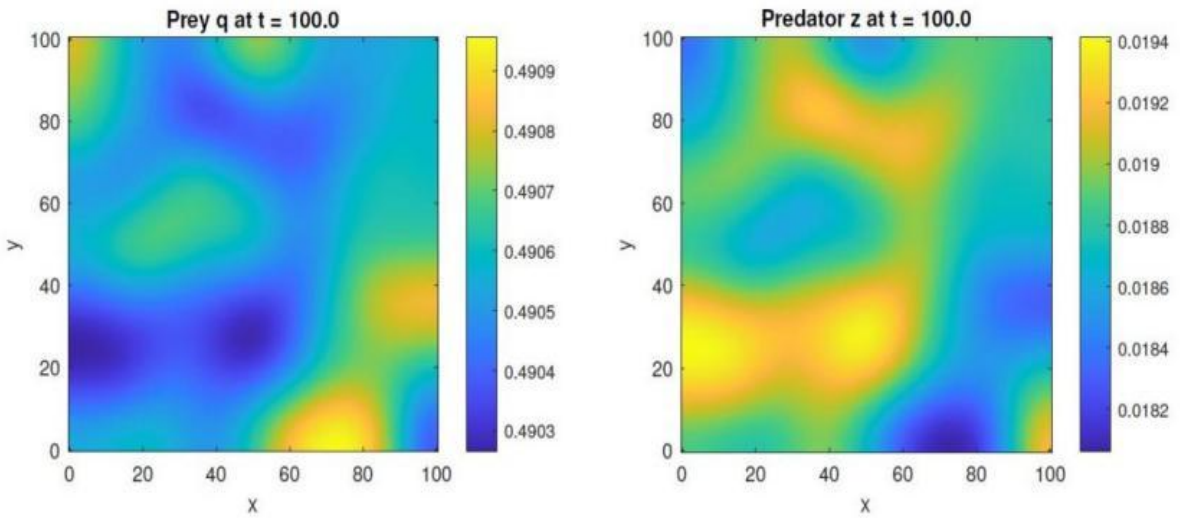

Note: Other parameters values; $m = 0.5, r_1 = 0.5$, $a_1 = 0.1$, $a_2 = 0.02$, $a_3 = 0.3$

The slight change in D_1 and D_2 reveals the progressive emergence of spatial distribution, in which the left plot in Figure 2 shows how fast the prey responds to changes in the predators' diffusion rate. Prey are seen in isolated patches, avoiding high predation together with some prey in refuge, resulting from a moderate refuge rate of $m = 0.5$, which makes it difficult for predators to access them. The left plot in figure 2 with ($t = 100$), prey distribution showed some faint patchiness with yellow-orange hues indicating prey aggregations, while blue-green regions of lower density, reflecting initial responses to predation pressure under moderate harvesting ($r_1 = 0.5$). Concurrently, in the right plot, predators exhibit scattered high-density clusters in yellow tones, slightly out of phase with prey peaks, indicating their fast dispersal under ($D_2 = 0.2$) and active foraging behavior. As time progresses, these patterns sharpen significantly, in which prey form more defined high-density zones of concentrated orange cores, while predator clusters become tighter and better aligned, highlighting enhanced spatial zones along prey species. The system settles into a stable configuration of well separated spot patterns, prey organize into isolated hotspots surrounded by low density backgrounds, visualized through strong contrast between central yellow regions and peripheral blue areas, while predators aggregate into corresponding dense patches, maintaining coexistence through balanced predation efficiency ($a_1 = 0.1$), low mortality ($a_2 = 0.02$), strong intraspecific competition ($a_3 = 0.3$) and slight increase in diffusion from $D_1 = 0.1$, $D_2 = 0.2$ to $D_2 = 0.5$. When diffusion rates increased to $D_1 = 0.2$ and $D_2 = 0.5$, the system evolved faster, and at $t = 500$, it reaches homogeneous state where prey stabilize tightly around $[0.492095 - 0.49212]$ and predators fluctuate narrowly, suggesting a stable distribution maintained by ecological balance and there were no further changes in prey and predator distributions.

Figure 3

Spatiotemporal Distribution of Predator and Prey with $D_1 = 0.2$ *and* $D_2 = 0.5$ *and* $t = 500$.

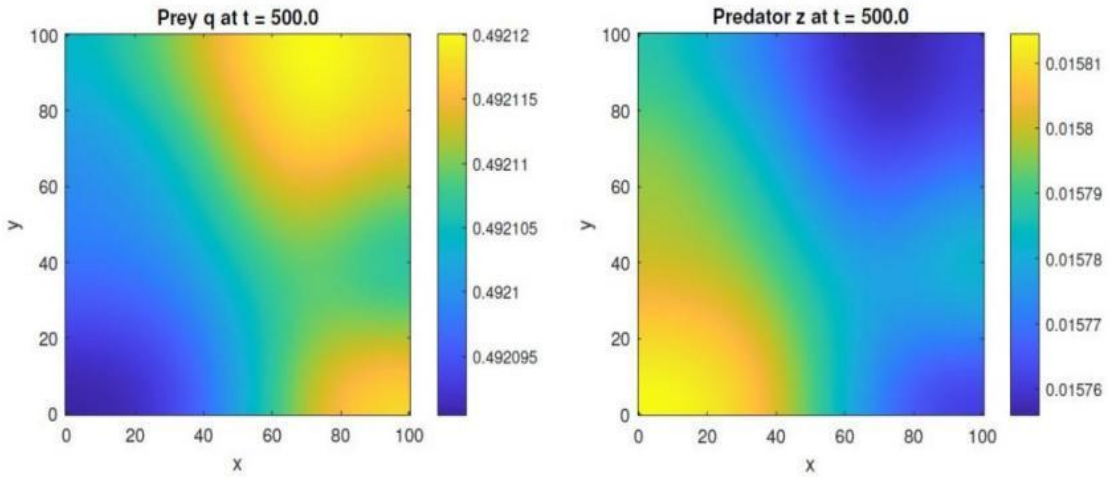

Note: Other parameter values used; $m = 0.5$, $r_1 = 0.5$, $a_1 = 0.1$, $a_2 = 0.02$, $a_3 = 0.3$

Turing pattern formation

Turing pattern formation is a fundamental mechanism in spatial ecology that explains how uniform, homogeneous states can break symmetry to form stable, complex spatial structures such as spots and stripes. This phenomenon arises in reaction-diffusion systems where interacting species diffuse at different rates across space. In this model, Turing patterns emerge when predators diffuse significantly faster than prey ($D_2 > D_1$), destabilizing the stable coexistence equilibrium E_2.

Although deriving explicit analytical thresholds for Turing instability is mathematically intractable in the current PDE model due to the nonlinear dependence of equilibrium densities on refuge (m), harvesting(r_1) and competition (a_3) parameters, the numerical simulations robustly demonstrate that diffusion-driven pattern formation occurs consistently when $D_2 > D_1$ .This empirical finding aligns with both classical Turing theory which requires differential diffusion rates and recent ecological modeling studies (Wang *et al*., 2011; Liu *et al*., 2019; Han *et al*., 2021). The systematic emergence of spots and stripes under $D_2 > D_1$ combined with ODE stability at $E_2((Tr(J) < 0,\ Det(J) > 0)$ provides strong numerical evidence that the condition $D_2 > D_1$ acts as predictor of spatial self-organization on this harvested predator-prey system with prey refuge and intraspecific competition .

The process begins with both populations distributed nearly uniformly across the domain, initialized close to their equilibrium densities. As shown in Figure 4 panels (*a*−*f*), even small random perturbations introduced can break perfect symmetry and lead to instability. These initial fluctuations are minor, but they trigger a local increase in prey density that finally attracts fast-moving predators, which migrate into these blues with prey regions from surrounding areas. However, this predation suppresses prey growth locally while simultaneously depleting the predator population due to intraspecific competition and mortality.

Over time, these interactions lead to the self-organized formation of distinct high and low density regions. By $t = 500$, the system exhibits early stage patterns for moderate refuge rate ($m = 0.5$) in Figure 4 (*a*) while advancing to more defined patterns in panels (*c, d*) with high refuge rate of $m = 0.7$ and $m = 0.9$ respectively, all under low predator diffusion of ($D_2 = 0.1$). In Figure 4, panels (*b, d, f*), well-defined structures start appearing as D_2 increases to 0.5 here, larger and more defined patches emerge. At higher refuge levels ($m = 0.7, 0.9$), the patterns become increasingly intricate and fragmented, reflecting the interplay between reduced predation pressure and enhanced dispersal.

Figure 4

Turing Patterns Showing Predators Distribution in Yellow Zones and Prey Distribution in Blue Zones at t =500.

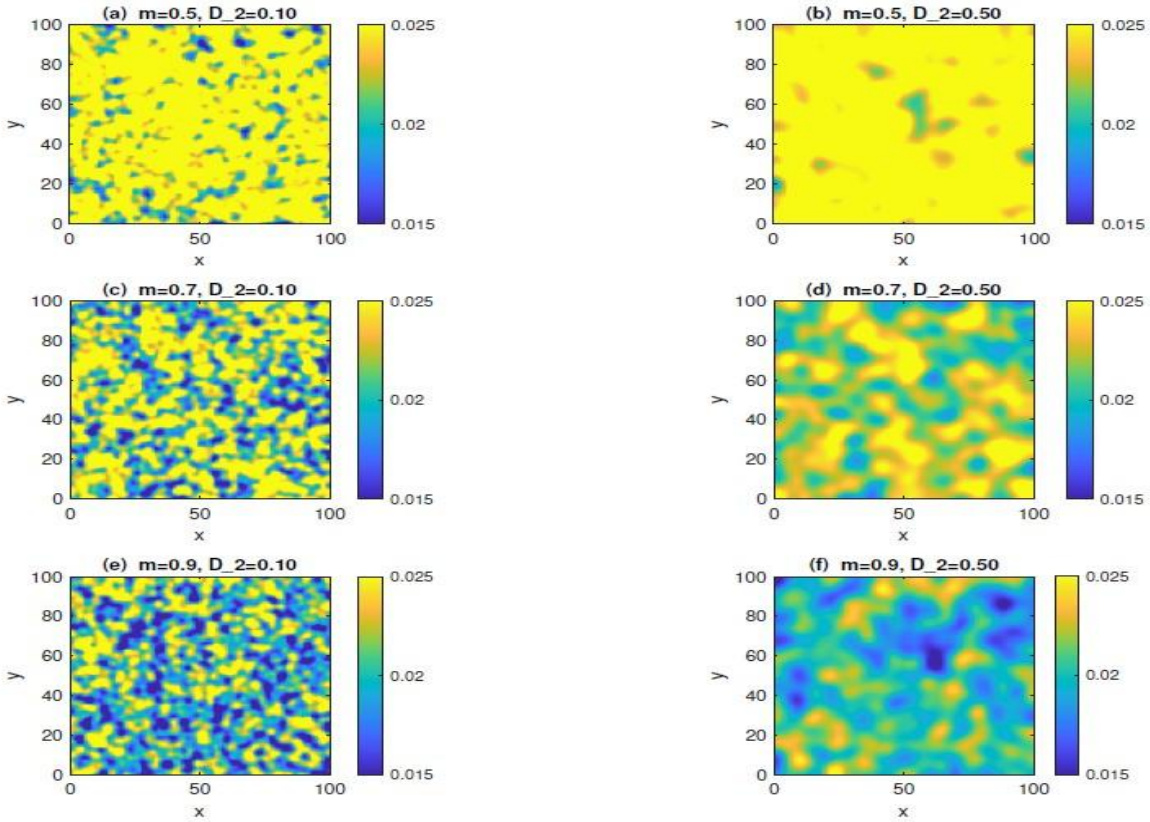

Note: Parameter values used; m = (0.5,0.7,0.9),r_1 = 0.5,D_1 = 0.1,D_2 = (0.1,0.5),a_1 = 0.1,a_2 = 0.02,a_3 = 0.3

Furthermore; when t = 1000 in Figure 5, the patterns matured into well-defined and stable configurations with no further changes. Panel (*a*) and (*b*) show spotted structures in Figure 5, while panel (*c*) to (*f*) demonstrate how very high diffusion (D_2 = 0.9) together with high refuge rate can homogenize the field by forming clear yellow zones of predator while prey being protected in the blue zones. These results visually confirm that pattern morphology is critically sensitive to the balance between prey refuge and predator mobility, offering an understanding of how ecological mechanisms shape biodiversity and resilience in spatially extended habitats.

Figure 5

Turing Patterns Showing Predators Distribution in Yellow Zones and Prey Distribution in Blue Zones at t =500

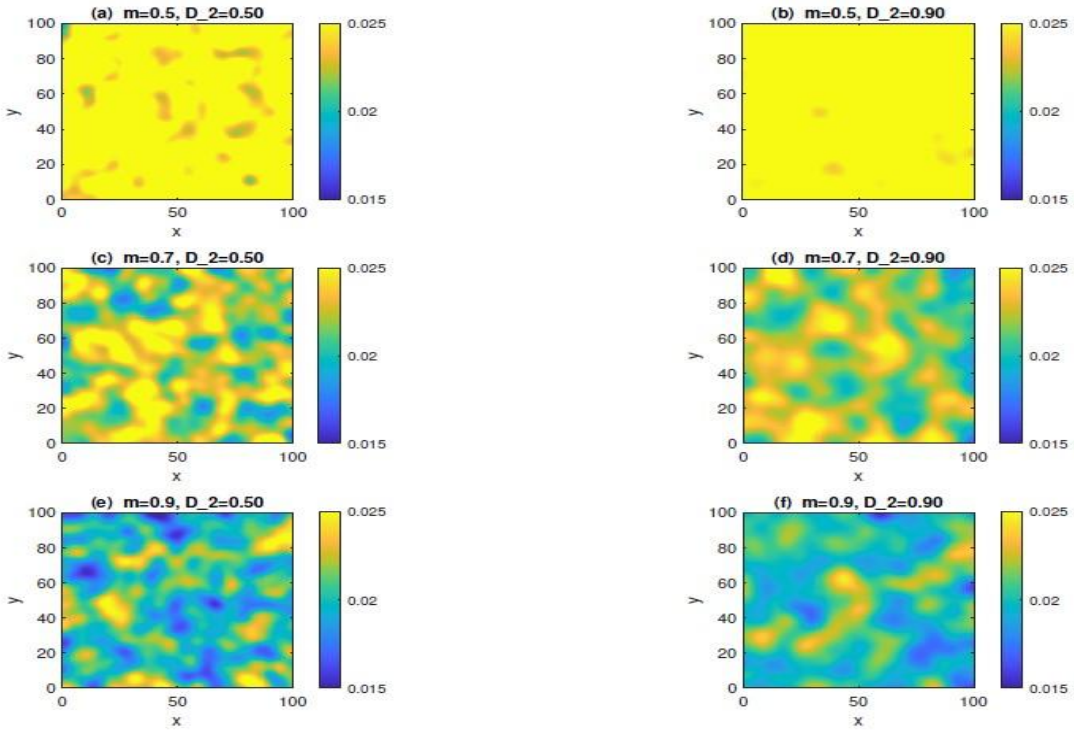

Note: Parameter values used; m = (0.5,0.7,0.9), r_1 = 0.5, D_1 = 0.1, D_2 = (0.5,0.9), a_1 = 0.1, a_2 = 0.02, a_3 = 0.3

Discussion

Comparison and quantitative interpretation of numerical Simulations.

This study extended the non-spatial predator–prey model of Mapunda and Sagamiko (2021) by incorporating spatial diffusion, thereby enabling the analysis of spatiotemporal pattern formation in a harvested system with prey refuge and intraspecific competition among predators. The results demonstrated that the interplay between refuge rate (m), harvesting intensity (r_1), and differential diffusion coefficients (D_1 and D_2) critically governs both local stability and large-scale spatial organization.

Analytically, the coexistence equilibrium E_2 is locally asymptotically stable in the absence of diffusion when $(1-m)(1-r_1)a_1 > a_2$, confirming that sufficient prey availability regulated by refuge and harvesting is necessary to sustain predator populations. However, while Mapunda and Sagamiko (2021) identified the refuge level m as the primary bifurcation parameter showing that predator extinction occurs when $m > 0.78$ due to insufficient prey accessibility, the spatial framework developed in this study reveals that even at moderate refuge levels ($m = 0.5$), spatial heterogeneity can emerge through Turing instability when $D_2 > D_1$. The results indicate that high refuge ($m = 0.9$) does not necessarily lead to predator extinction in spatial settings, as observed in the non-spatial model, instead, it suppresses pattern formation and promotes near-homogeneous coexistence, especially when combined with high predator diffusion ($D_2 = 0.9$). This suggests that spatial mobility can reduce destabilizing effects of excessive refuge a phenomenon which is invisible in ODE-based system.

Numerical simulations confirmed that small random perturbations around E_2 grow into self-organized spot patterns by $t = 1000$ under baseline parameters ($m = 0.5$, $r_1 = 0.5$, $D_1 = 0.1$, $D_2 = 0.2$ Figure 4). Increasing D_2 accelerated pattern formation with well-defined spots emerge as early as $t = 100$ when $D_2 = 0.5$ (Figure 2), whereas very high diffusion ($D_2 = 0.9$ with $D_1 = 0.3$) led to rapid homogenization by $t = 500$ (Figure 3). At moderate refuge ($m = 0.5$), predation pressure drives clear spatial segregation (Figures 1 and 4), but at higher refuge levels ($m = 0.7$

and $m = 0.9$), reduced predation weakened feedback mechanisms necessary for pronounced patterning. Notably, when $m = 0.9$ and $D_2 = 0.9$, the system approached a near-homogeneous state by $t = 1000$ (Figure 5 panel f), indicating that high refuge reduces spatial destabilization even under fast predator diffusion. Thus, while the non-spatial model of Mapunda and Sagamiko emphasizes demographic thresholds for extinction, the spatial model presented in this study uncovered how diffusion and refuge jointly regulate not only persistence but also the spatial coexistence highlighting that ecosystem resilience in real landscapes depends on both local interactions and spatial redistribution processes.

Figures (1-5) visualized the spatiotemporal dynamics described above, with parameter values from Table 2. Figure 1 with (D_1=0.1, D_2=0.2, t=50) showed initial pattern emergence, where prey form incipient hotspots ($q_{max} \approx 0.52$) and predators aggregate into scattered clusters ($z_{max} \approx 0.11$). Figure 2 (D_1=0.2, D_2=0.5, t=100) demonstrated accelerated segregation under higher diffusion ratio $\left(\frac{D_2}{D_1}=2.5\right)$, with prey amplitude $A_q \approx 0.18$ and predator amplitude $A_z \approx 0.06$. Figure 3 (**t = 500**) confirms pattern stabilization, with densities converging to $q \in [0.492095, 0.492120]$ and $z \in [0.0946, 0.0948]$. Figures 4-5 which systematically vary refuge (m=0.5, 0.7,0.9) and predator (D_2=0.1, 0.5,0.9), revealed that the moderate refuge (m=0.5) optimizes heterogeneity ($A_q \approx 0.156$), while (m=0. 9) suppresses patterns ($A_q \approx 0.0.034$), particularly when combined with fast diffusion (D_2=0.9). These visualization quantitatively confirm that differential mobility ($D_2 > D_1$) drives Turing instability, refuge modulates pattern intensity.

Conclusion

In this work, spatiotemporal predator-prey model characterized by a system of differential equations (PDEs) incorporating reaction and diffusion was studied. The extensive numerical analysis was done successfully to validate analytical investigation. It was observed that, pattern generation is affected by varying parameters such as prey refuge (m) and diffusion coefficients (D_1, D_2). The outcomes included the creation of intricate spatiotemporal patterns and finally it was

observed that at high refuge rate m = 0.9 and predator diffusion rate above D_2 = 0.9, the system displayed stable Turing patterns. The spatial complexity attained in reaction-diffusion systems included spots and stripes structures that emerge due to diffusion-driven instability. Through simulations using the IMEX Euler method, we demonstrated the transition from uniform coexistence to self-organized spatial heterogeneity when predators diffuse faster than prey ($D_2 > D_1$), confirming the occurrence of Turing instability near the coexistence equilibrium E_2.

The investigation of spatiotemporal predator-prey model provided important understanding of the spatial organization and stability of ecological systems. In particular, the study revealed that increasing predator diffusion enhances spatial aggregation while decreasing the refuge level intensifies predation pressure and accelerates pattern formation.

Thus, these discoveries have practical applications in sectors such as conservation biology, pest control, and biodiversity protection. Therefore, studying spatial distributions and Turing patterns in spatiotemporal predator-prey models is an important area of study in ecological system. Further research into the mechanics and consequences of Turing patterns in predator-prey dynamics will surely contribute to a better understanding of the complex interplay between species interactions and geographical variability.

Recommendations

Based on the findings of this study, conservation and ecosystem management strategies should prioritize the regulation of prey refuge levels and account for species-specific diffusion rates to promote stable and spatially structured coexistence. Simulation results demonstrated that moderate refuge levels $m = 0.5$ facilitates the emergence of well-defined Turing patterns such as spots and stripes by maintaining sufficient predation pressure while protecting a portion of the prey population. These self-organized spatial heterogeneity enhance ecological resilience by preventing population collapse and supporting biodiversity. In contrast, high refuge levels such as $m = 0.9$ suppresses spatial patterning and drive the system toward homogeneity, particularly when combined with high predator diffusion (D_2 = 0.9), potentially reducing habitat complexity and adaptive capacity. Furthermore, pattern formation consistently occurs only when predators diffuse faster than prey ($D_2 > D_1$), confirming that differential mobility is a key driver of spatial organization. Therefore, protected area design, corridor planning and habitat restoration efforts should incorporate both refuge provision and movement dynamics ensuring that predator and prey dispersal traits are considered alongside shelter availability. Such an integrated approach will support the long-term persistence of harvested predator–prey systems in spatially heterogeneous environments.

Acknowledgment

The authors would like to express their sincere gratitude to the Department of Mathematics for providing the academic environment and resources that made this research possible. We are deeply thankful for the support and guidance received throughout the course of this study. We would also appreciate Eastern Africa Universities Mathematics Programme (EAUMP) for their partial sponsorship that facilitated this study.

References

Agape, K., Ndesendo, V. M. K., & Begum, S. (2021). Screening of Aflatoxin-Producing Fungi in Maize and Groundnuts from Three Regions in Tanzania. *Tanzania Journal of Science,* 47(2), 609–615. https://doi.org/10.4314/tjs.v47i2.16

Berryman, A. A. (2000). Spatial dynamics of predator–prey interactions: The role of refuges and dispersal. Ecology Letters, 3(6), 363–369. https://doi.org/10.1046/j.1461-0248.2000.00160.x

Cosner, C. (2004). The effects of spatial heterogeneity on population dynamics. In Proceedings of the Royal Society of London. Series B: Biological Sciences (Vol. 271, pp. 1–12).

Das, U., Kar, T. K., & Pahari, U. K. (2013). Global dynamics of an exploited prey–predator model with constant prey refuge. International Scholarly Research Notices: Biomathematics, 2013, Article 562907. https://doi.org/10.1155/2013/562907

Han, R., Guin, L. N., & Dai, B. (2021). Consequences of refuge and diffusion in a spatiotemporal predator–prey model. Nonlinear Analysis: Real World Applications, 60, Article 103281. https://doi.org/10.1016/j.nonrwa.2021.103281

Han, R., Li, Y., Liu, H., & Dai, B. (2022). Dynamical response of a reaction-diffusion predator–prey system with cooperative hunting and prey refuge. Journal of Statistical Mechanics: Theory and Experiment, 2022(10), 103501. https://doi.org/10.1088/1742-5468/ac97a5

Kar, T. K. (2005). Stability analysis of a prey–predator model incorporating a prey refuge. Communications in Nonlinear Science and Numerical Simulation, 10(6), 681–691. https://doi.org/10.1016/j.cnsns.2003.08.006

Kumar, K. (2006). Modelling and analysis of a harvested prey–predator system incorporating a prey refuge. Journal of Computational and Applied Mathematics, 185(1), 19–33.

https://doi.org/10.1016/j.cam.2005.01.012
Liu, H., Wang, J., & Wei, J. (2019). Pattern formation in a reaction–diffusion predator–prey model with weak Allee effect and delay. Complexity, 2019, Article 9831231. https://doi.org/10.1155/2019/9831231
Majeed, A. A. (2018). The dynamics of a prey–predator model with prey refuge and stage structures in both populations. Science International (Lahore), 30(3), 461–470.
Mapunda, A., Mureithi, E., Shaban, N., & Sagamiko, T. (2018). Effects of over-harvesting and drought on a predator–prey system with optimal control. Open Journal of Ecology, 8(8), 459–482. https://doi.org/10.4236/oje.2018.88029
Mapunda, A., & Sagamiko, T. (2021). Mathematical analysis of a harvested predator–prey system with prey refuge and intraspecific competition. Tanzania Journal of Science, 47(2), 101–115. https://doi.org/10.4314/tjs.v47i2.10
Mohd, S., Noorani, M. S. M., & Hashim, I. (2012). Pattern formation in a two-dimensional space-diffusive prey–predator model. Journal of Applied Sciences, 12(19), 2016–2025. https://doi.org/10.3923/jas.2012.2016.2025
Quan, H., Zhang, X., & Liu, Z. (2023). Dynamics of a predator–prey model with impulsive diffusion and transient/nontransient impulsive harvesting. Mathematics, 11(14), Article 3254. https://doi.org/10.3390/math11143254
Sharmila, S., Gunasundari, V., & Rajagopal, K. (2023). Spatiotemporal dynamics of a reaction-diffusive predator–prey model: A weak nonlinear analysis. International Journal of Differential Equations, 2023, Article 6687625. https://doi.org/10.1155/2023/6687625
Sharmila, S., & Gunasundari, V. (2023). Mathematical analysis of prey–predator models with Holling type I functional responses and time delay. Communications in Mathematical Biology and Neuroscience, 2023, Article 62. https://doi.org/10.28919/cmbn/7856.
Wang, J., Shi, J., & Wei, J. (2011). Dynamics and pattern formation in a diffusive predator–prey system with strong Allee effect in prey. Journal of Differential Equations, 251(4–5), 1276–1304. https://doi.org/10.1016/j.jde.2011.03.023